

## A Practical Approach for Estimating Drag Increase due to Volume Increase in the Center Body of a High-Speed UAV

Ugur Ozdemir<sup>1\*</sup>

<sup>1</sup> Department of Flight Training, Faculty of Aeronautics And Astronautics, Eskisehir Technical Universtiy, Eskisehir  
\* [ugurozdemir@eskisehir.edu.tr](mailto:ugurozdemir@eskisehir.edu.tr)

(Geliş/Received: 17/02/2024;

Kabul/Accepted: 03/09/2024)

**Abstract:** High-speed unmanned aerial vehicles are used for many purposes in aviation. High-speed aircraft do not only fly at supersonic speed, but their subsonic flight performance is also important. Aircraft design is an iterative process in which many disciplines work together. The design process is updated by the negotiation of different disciplines. There may be a demand for a body volume increase in the interior design process. The increase in volume can be achieved by the elongation or expansion of the body. A volume increase in the center body causes an increase in drag. The aim of this study is to predict the effect of the elongation or expansion of the center body on drag in a practical way. It is investigated using a structure proposed with MATLAB and DATCOM. The results in both subsonic and supersonic regimes are formalized separately and compared. It is shown that in case of providing the same volume increase in both subsonic and supersonic regimes, the elongation of the aircraft center body causes less drag compared to widening.

**Keywords:** Drag estimation, Digital DATCOM, high-speed UAV.

### Yüksek Hızlı İHA'nın Gövde Hacim Artışı Nedeniyle Sürüklenme Kuvvetinin Artışının Tahmininde Pratik Bir Yaklaşım

**Öz:** Yüksek hızlı insansız hava araçları havacılıkta birçok amaç için kullanılmaktadır. Hızlı uçaklar sadece süperonik hızda uçmazlar, aynı zamanda süperonik altı uçuş performansı da önemlidir. Uçak tasarımı, birçok disiplinin birlikte çalıştığı iteratif bir süreçtir. Tasarım süreci, farklı disiplinlerin müzakeresiyle güncellenir. İç tasarım sürecinde gövde hacminde bir artış talebi olabilir. Hacim artışı, gövdenin uzatılması veya genişletilmesiyle elde edilebilir. Merkezi gövde hacmindeki bir artış, sürüklenmede kuvvetinde bir artışa neden olur. Bu çalışmanın amacı, merkezi gövdenin uzatılması veya genişletilmesinin sürüklenme kuvveti üzerindeki etkisini pratik bir şekilde öngörmektir. MATLAB ve DATCOM yazılımları kullanılarak oluşturulan bir yapı ile bu durum incelenmiştir. Süperonik ve süperonik altı rejimlerde elde edilen sonuçlar ayrı ayrı formalize edilmiş ve karşılaştırılmıştır. Aynı hacim artışının süperonik ve süperonik altı rejimlerde sağlanması durumunda, uçağın merkezi gövdesinin uzatılmasının genişlemeye kıyasla daha az sürüklenme kuvvetine neden olduğu gösterilmiştir.

**Anahtar Kelimeler:** Sürüklenme kuvveti kestirimi, Digital DATCOM, yüksek hızlı İHA.

#### 1. Introduction

Currently, the principal ways to obtain aerodynamic parameters are a wind tunnel test, Computational Fluid Dynamics (CFD) analysis, and semi-empirical methods [1]. Wind tunnels are assuring and classical ways to determine the derivatives. However, they are time-consuming and costly processes. Therefore, they are not recommended for the initial phase [1-3]. CFD software can model aircraft with a more complex structure. However, the software parameters are intricate, and its computer processor demands are immense [1,4]. Different aerodynamic flow models can be applied to obtain flow field properties. The Navier–Stokes equations are the main flow models representing viscous, rotational, and compressible flows [5,6]. Different approaches can be listed as follows: DATCOM, XFLR, TORNADO, AVL, PANAIR, ANSYS, etc. Each software has its restrictions limiting its application areas. The results obtained by TORNADO are precise only for slight angles of attack. It cannot cope with high Mach number conditions properly [7]. Athena Vortex Lattice (AVL) software is suitable for thin airfoils. Moreover, it is not convenient for small angles of attack and sideslip. ANSYS includes two modules, FLUENT and CFX, and it is a successful way to reveal stability and control characteristics. On the other hand, it includes a complex mesh generation process and lasts for many hours [5]. Alternatively, the commonly used technique in the early phase of aerodynamic estimations is semi-empirical methods [1]. These methods use datasheets, linear aerodynamic theory, and empirical equations to obtain aerodynamic parameters. DATCOM [8,9], also known as Missile DATCOM, is a widely used one. It was created by the US Air Force Research Laboratory and is now in the public domain. In academia, it has found a place as one of the trustworthy instruments to determine the stability and control derivatives of an aircraft [5]. It has been consistently modified with new test

\* Corresponding author: [ugurozdemir@eskisehir.edu.tr](mailto:ugurozdemir@eskisehir.edu.tr) ORCID Number of author: 1 0000-0001-7969-7717

data and novel computational analysis options [10-12]. DATCOM is extensively employed for aircraft planes, airships, projectiles, missiles, etc. The software combines the wind tunnel test data with durable flexibility and high accuracy [12]. Although this kind of methods cannot entirely replace wind tunnel tests and CFD analysis, they can lower time costs enormously [1]. Aerodynamic calculations on individual wings, aircraft body and wing-body [13-17], and deformable wing or a swept-wing aircraft [18-22] are executed using DATCOM. A new approach for aerodynamic shape optimization is used in Ref. [23], where CFD and DATCOM are used together. In this way, the researchers manage to decrease the necessary CFD calls by over 62.5%.

An empirical method to estimate the hydrodynamic derivatives of streamlined undersea vehicles is used in Ref. [24]. They show that DATCOM outputs are compatible with the results from other sources. The state-space model extraction of a high wing design UAV is proposed in Ref. [25] using DATCOM for a fairly accurate plant model.

The longitudinal dynamic system modeling of a fixed-wing UAV is performed using both flight test data and DATCOM calculations in Ref. [26], which demonstrates that both approaches provide a similar result. DATCOM is used in several studies and validated with flight test data [26-27]. Unguided rolling projectiles at varying Mach numbers are studied in Ref. [28] using DATCOM. Digital DATCOM is also used to obtain the aerodynamic characteristics of UAV for the development of a pitch control subsystem for a fixed-wing UAV in Ref. [29]. Moreover, it is used to analyze the aerodynamic performance during the folding process of wing-tip [30].

Aircraft design is an iterative process in which many disciplines work together [33]. The design process is updated by the negotiation of different disciplines. There may be a demand for a body volume increase in the interior design process. The increase in volume can be achieved by the elongation or expansion of the body. In addition, this volume increase should be in the center body, which is convenient to equip the system and place useful loads. A volume increase in the center body will cause an increase in drag. This directly changes the required thrust-available thrust graph and may cause the need for a new engine.

The effect of the elongation and expansion of the aircraft center body on drag in both subsonic and supersonic regimes can be addressed by methods such as the flight test and CFD mentioned above. However, these methods are time-consuming and not economical. Methods that will produce fast and reliable results are required, especially in projects with time constraints. The purpose of this study is to provide a structure to meet the aforesaid need. DATCOM software, which is especially validated for classical aircraft configurations, was used in this study. Investigating the reliability of DATCOM software is beyond the scope of this article, as it has been researched in many studies before. This article is built on the knowledge in the literature that DATCOM software is reliable for classical geometries. The input files required by DATCOM software for each geometry change were automatically created with the code developed using MATLAB software. At the same time, DATCOM output files were drawn by the program developed using MATLAB software. First, the creation of a reference UAV geometry in DATCOM was given. Then, three different volume increases were considered as both the elongation of the center body and the widening of the center body. Each geometry change was analyzed with the proposed MATLAB-DATCOM structure. As a result, an approach was put forward to predict the drag increase.

## 2. Materials and Methods

Wind tunnel and flight testing, CFD, and semi-empirical methods can be used to calculate aerodynamic parameters. Digital DATCOM was used in this paper. It was first introduced in 1960 and improved in 1978. It is an approach combining theoretical and experimental procedures and provides reliable results for standard aircraft configurations. DATCOM has an algorithm to obtain aerodynamic parameters, i.e., stability and control derivatives, either by the extrapolation or interpolation of data from the US Air Force for years [5,43]. The structure of DATCOM is as follows: 1) Defining an input file: aircraft shapes and the flight environment, 2) Executing the main function to trigger DATCOM, 3) The software creates an output file by detecting the wind tunnel test data and a theoretical approach suitable for input parameters. It is often used in the first phase of aircraft development to evaluate different shape schemes [1].

In this study, the unmanned aerial vehicle geometry in Fig. 1 was used to show the effect of the elongation or expansion of the center body on drag.

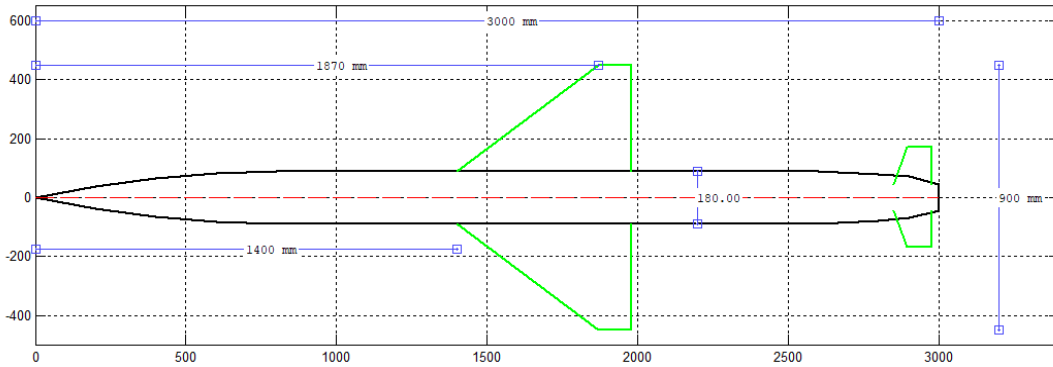


**Figure 1.** Top view of the UAV model.

The geometric parameters, along with flight conditions, are the basic and most important requirements for modeling an aircraft in any software.

Table 1 lists the flight conditions to be analyzed.

**Table 1.** Flight Conditions.

	Subsonic	Supersonic
Mach Number	M = 0.6	M = 1.4
Altitude	h = 3000 m	h = 3000 m
Angle of attack	$-6^\circ < \alpha < 20^\circ$	$-6^\circ < \alpha < 20^\circ$

While some geometric properties of the UAV are given in Table 2, the definitions of these sizes are given in Table 3.

**Table 2.** Flight Conditions.

SREF	234000 mm <sup>2</sup>
CBARR	255 mm
BLREF	900 mm
XCG	1748 mm
ZCG	0 mm
BNOSE	BNOSE = 2 ogive nose
BLN	800 mm
BLA	1800 mm

**Table 3.** Definition of the geometric abbreviations used in the analysis.

Variable Name	Definition
SREF	Planform area used as a reference area
CBARR	Value of the theoretical wing mean aerodynamic chord
BLREF	Value of the wingspan
XCG	Longitudinal distance of CG from the nose
ZCG	Vertical location of CG relative to the reference plane
BNOSE	BNOSE=1 conical nose; BNOSE = 2 ogive nose
BLN	Length of the body nose
BLA	Length of the cylindrical afterbody segment

In the DATCOM program, the body geometry is created by dividing it into segments. Accordingly, the airframe is divided into segments as in Fig. 2 using the values in Table 4.

**Table 4.** Dimensions of the body segments.

Station	1	2	3	4	5	6	7	8	9	10
X (mm)	0	200	400	600	800	1500	2600	2800	2900	3000
S (mm <sup>2</sup> )	0	4257	13454	21021	25447	25447	25447	20106	15394	6362
P (mm)	0	231.28	411.17	513.96	565.48	565.48	565.48	502.65	439.82	282.74
R (mm)	0	36.81	65.44	81.80	90	90	90	80	70	45

where X: Longitudinal distance measured from the arbitrary location; S: Cross-sectional area; P: Periphery at station x(i); R: Planform half width

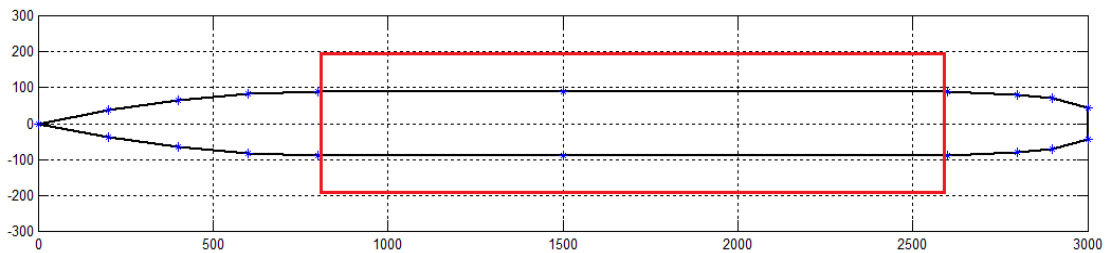


**Figure 2.** Segmentations of the body.

The cross-sectional area between segments 5 and 7 shown in the red box in Fig. 2 is equal. The distance between these two segments, which we call the center body, is 1800 mm, and values of the radius, circumference, and area remain constant between these two segments (Fig. 3). The center body is the most useful part of the aircraft fuselage as an interior layout. In this work, the elongation or expansion of the body will be performed in this region to create an additional volume. However, when analyzing the center body expansion, it will be taken into account that the front and rear parts will expand in proportion to this part.

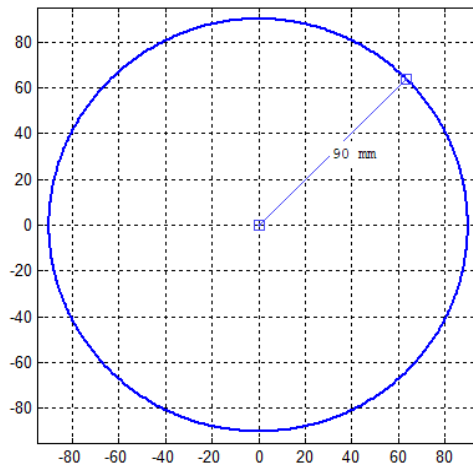


**Figure 3.** Cross-section on the constant body section.

The volume increase to be provided by the elongation or expansion of the center body (shown in Fig. 2 by the red rectangular) is calculated in Table 5. Accordingly, the 270-mm elongation of the body and the 6.51-mm increase in the radius of the body provide the same volume increase (4580 cm<sup>3</sup>). Hence, a 270-mm elongation corresponds to an extension of 6.51 mm in the radius. The same calculations were made in 15%, 25%, and 35%

increments of the center body length (the part with a fixed cross-sectional area of 1800 mm in length) and given in Table 5.

**Table 5.** Volume increase caused by the center body elongation or expansion.

Percent increase in the body (extension)	Equivalent increase in the radius to sustain the same volume	Volume increase
15% (270 mm)	7.24% (6.51 mm)	6871 cm <sup>3</sup>
25% (450 mm)	11.80% (10.62 mm)	11451 cm <sup>3</sup>
35% (630 mm)	16.16% (14.57 mm)	16032 cm <sup>3</sup>

To investigate whether the center body elongation or enlargement providing the same volume increase will be better, the conditions given in Table 4 should be analyzed and compared separately. This investigation will be made for both subsonic and supersonic flight regimes.



**Figure 4.** Digital DATCOM analysis process

First, the input file containing the flight geometry and flight conditions given in Tables 1 and 3 is prepared. After the Digital DATCOM program is run, the output file is created.

While the subsonic and supersonic analyses of a single geometry are performed as shown in Fig. 4, a different input file should be prepared for each of the different geometry changes, as in our problem.

As seen in Fig. 5, the MATLAB program was used to create the Input File as an iterative for each geometry change, to call the Digital DATCOM and to create the graphics from the output files.

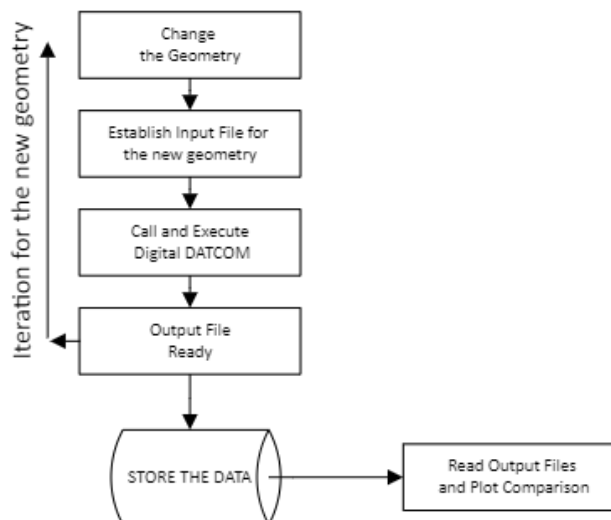


**Figure 5.** Iterative Digital DATCOM analysis process.

### 3. Results and Discussion

The following graphs were drawn using the data in the output files obtained for each geometry. The drag coefficient versus attack angle of the aircraft body given in Fig. 1 is drawn in Fig. 6. In Fig. 6, the change in the drag coefficient at both 0.6 Mach and 1.4 Mach according to the angle of attack is given. As expected, the drag coefficient is higher at supersonic speed than subsonic speed. Furthermore, while the variation in the drag coefficient with respect to the angle of attack ( $C_{D\alpha}$ ) is more linear at subsonic speeds ( $C_{D\alpha}$ ) (almost constant), it continues to increase in the supersonic regime. It is larger, especially at high angles of attack. Therefore, in supersonic drag calculations,  $C_{D\alpha}$  should be taken depending on the angle of attack.

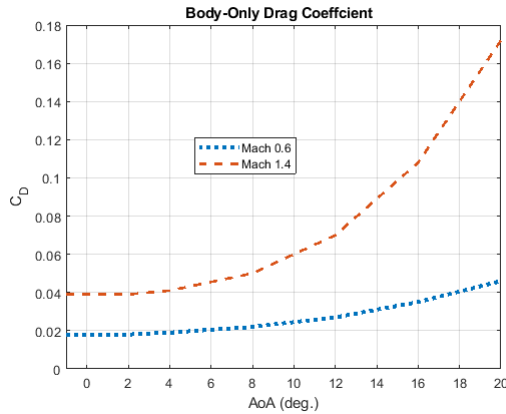


**Figure 6.** Body-only drag coefficient versus the angle of attack in the subsonic and supersonic regimes.

First, the effects of the elongation of the body with a constant cross-sectional area are shown in Fig. 7.

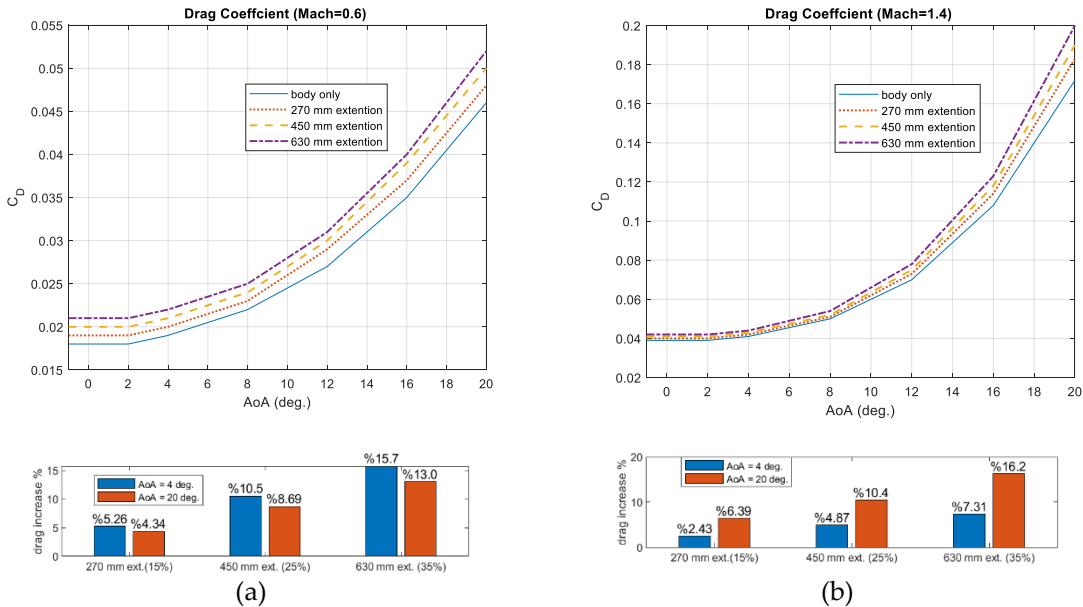


**Figure 7.** Body extension effect on the body-only drag coefficient in: **(a)** Subsonic regime (Mach=0.6), **(b)** Supersonic regime (Mach=1.4)

The effects of 270 mm (15%), 450 mm (25%), and 630 mm (35%) elongations of the center body are shown on the same graph, respectively. These elongations resulted in an increase in drag of 5.26%, 10.5%, and 15.5%, respectively, at a low angle of attack in the subsonic regime. Using these values, the drag effect of the percent elongation in the center body at a low angle of attack in the subsonic regime can be expressed as a 3rd-order equation as in Eq. 1:

$$\% \delta D = -0.0002 \% \delta L^3 + 0.0162 \% \delta L^2 + 0.1595 \% \delta L \quad (1)$$

where

$\% \delta D$ : percent drag increase, i.e., the result value of 5 means a 5% increase

$\% \delta L$ : percent elongation of the center body, between 0 and 35

They also resulted in an increase in drag of 4.34%, 8.69%, and 13%, respectively, at a high angle of attack in the subsonic regime. Using these values, the drag effect of the percent elongation in the center body at a high angle of attack in the subsonic regime can be expressed as a 3rd-order equation as in Eq. 2:

$$\% \delta D = -0.0002 \% \delta L^3 + 0.0127 \% \delta L^2 + 0.1374 \% \delta L \quad (2)$$

These elongations resulted in an increase in drag of 2.43%, 4.87%, and 7.31%, respectively, at a low angle of attack in the supersonic regime. Using these values, the drag effect of the percent elongation in the center body at a low angle of attack in the supersonic regime can be expressed as a 3rd-order equation as in Eq. 3:

$$\% \delta D = -0.0001 \% \delta L^3 + 0.0070 \% \delta L^2 + 0.0777 \% \delta L \quad (3)$$

We can conclude an increase in drag of 6.39%, 10.40%, and 16.20%, respectively, at a high angle of attack in the supersonic regime. Using these values, the drag effect of the percent elongation in the center body at a high angle of attack in the supersonic regime can be expressed as a 3rd-order equation as in Eq. 4:

$$\% \delta D = -0.0003 \% \delta L^3 - 0.0124 \% \delta L^2 + 0.5476 \% \delta L \quad (4)$$

The effect of body elongation on drag is similar in the subsonic regime at both low and high angles of attack (i.e., percent drag increases at low and high angles of attack are close to each other). On the other hand, the percent drag increase values at low and high angles of attack in the supersonic regime are different.

In the supersonic regime, the percent drag increase at low angles of attack is almost half the increase at high angles of attack. For instance, while the 630-mm elongation of the center body at Mach 1.4 (a 35% increase in the body length) causes a 7.31% increase in drag at a low angle of attack, it causes a 16.2% increase at a high angle of attack (AoA = 20 deg.).

On the other hand, the percentage drag increase in the subsonic regime is 15.7% and 13.0% at low and high angles of attack, respectively. In the subsonic regime, in contrast to the supersonic regime, the percentage drag increase at high angles of attack is lower than the increase at low angles of attack. In case of a 630-mm (35%) body extension, the maximum body drag coefficient ( $C_D = 0.2$ ) is reached in the supersonic regime at an angle of attack of 20 deg. In case of body elongation, the most significant percent drag increase occurs at a high angle of attack in the supersonic regime. The effect of increasing the radius of the center body to drag is shown in Fig. 8. The effect of increasing the body radius of 6.51 mm (7.24%), 10.62 mm (11.80%), and 14.57 mm (16.16%) is shown on the same graph, respectively.

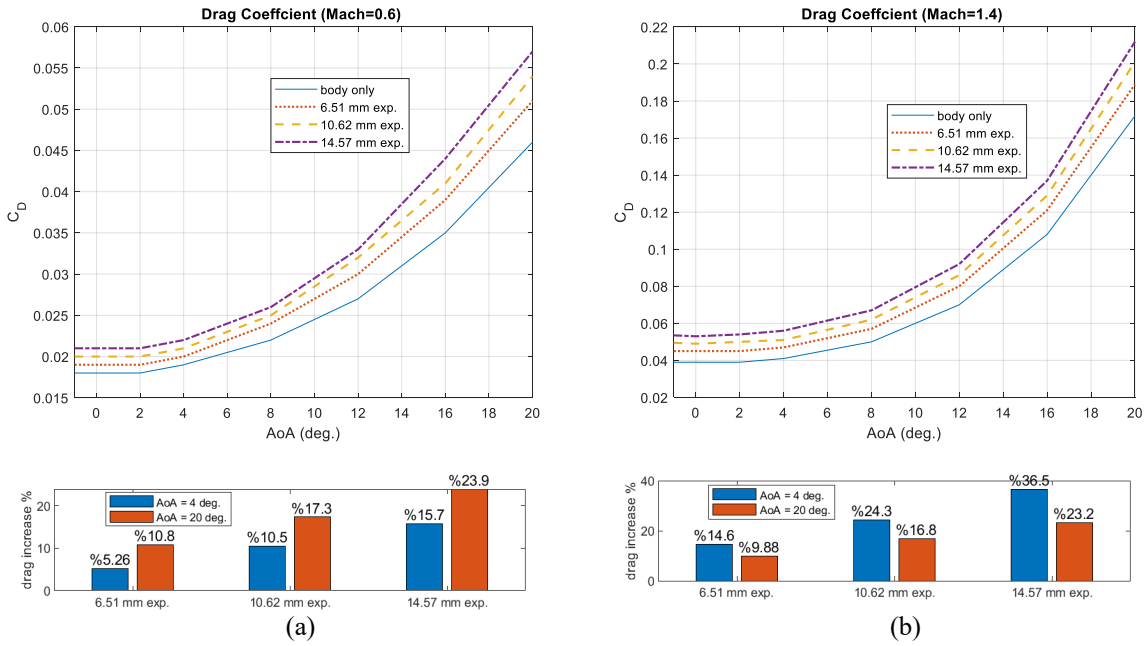


**Figure 8.** Body expansion effect on the body-only drag coefficient in: (a) Subsonic regime (Mach=0.6), (b) Supersonic regime (Mach=1.4)

These expansions resulted in an increase in drag of 5.26%, 10.5%, and 15.7%, respectively, at a low angle of attack in the subsonic regime. Using these values, the drag effect of the percent increase in the radius of the center body at a low angle of attack in the subsonic regime can be expressed as a 3rd-order equation as in Eq. 5:

$$\% \delta D = -0.0019 \% \delta r^3 + 0.0723 \% \delta r^2 + 0.3037 \% \delta r \quad (5)$$

where

$\% \delta D$ : percent drag increase, i.e., the result value of 5 means a 5% increase

$\% \delta r$ : percent elongation of the center body, between 7.24 and 16.16

These expansions in the center body also resulted in an increase in drag of 10.80%, 17.30%, and 23.90%, respectively, at a high angle of attack in the subsonic regime. Using these values, the drag effect of the percent increase in the radius of the center body at a high angle of attack in the subsonic regime can be expressed as a 3rd-order equation as in Eq. 6:

$$\% \delta D = 0.0010 \% \delta r^3 - 0.0239 \% \delta r^2 + 1.6144 \% \delta r \quad (6)$$

This resulted in drag increases of 14.60%, 24.30%, and 36.50%, respectively, at low angles of attack in the supersonic regime. Using these values, the drag effect of the percent increase of the body radius at a low angle of attack in the supersonic regime can be expressed as a 3rd-order equation (Eq. 7):

$$\% \delta D = 0.0041 \% \delta r^3 - 0.0682 \% \delta r^2 + 2.2968 \% \delta r \quad (7)$$

This resulted in drag increases of 9.88%, 16.80%, and 23.20%, respectively, at high angles of attack in the supersonic regime. Using these values, the drag effect of the percent increase of the body radius at a high angle of attack in the supersonic regime can be expressed as a 3rd-order equation (Eq. 8):

$$\% \delta D = -0.0011 \% \delta r^3 + 0.0348 \% \delta r^2 + 1.1729 \% \delta r \quad (8)$$



The effect of body expansion on drag at low and high angles of attack differs in both subsonic and supersonic regimes. In case of body expansion, the most significant percent drag increase occurs at a low angle of attack in the supersonic regime (Fig. 8b). When the body radius was widened by 14.51 mm, the maximum body drag coefficient reached  $C_D = 0.21$  at a 20-deg angle of attack in the supersonic regime. Equations 1-8 can be used to predict the drag effect of the elongation of the fuselage geometry or the increase in the radius of its cross-section, especially for aircraft with a similar geometry. To increase the volume of the aircraft fuselage by 6871 cm<sup>3</sup>, an extension of 6.51 mm in the fuselage length or 6.51 mm in the radius of the fuselage is required. The drag effect of these geometry changes, which will provide the same volume increase, is shown in Fig. 9.

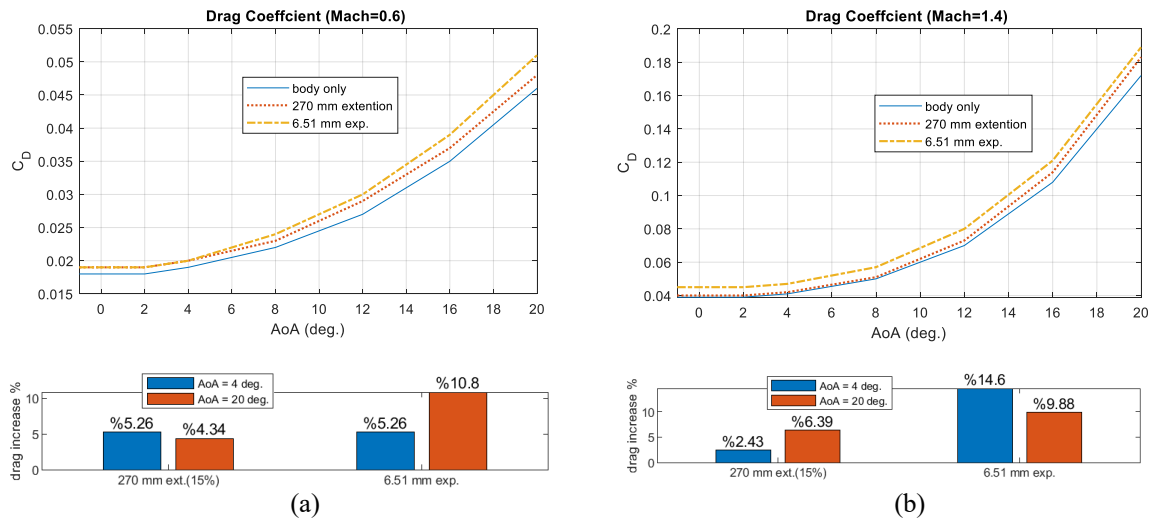


**Figure 9.** The influence of the 270-mm extension of the body length or the 6.51-mm expansion of the cross-section radius on the body-only drag coefficient in: (a) Subsonic regime (Mach=0.6), (b) Supersonic regime (Mach=1.4)

In the subsonic regime, while the 270-mm (15%) elongation of the center body at low angles of attack causes a 5.26% increase in body drag, the 6.51-mm widening of the radius of the center body cross-section causes an increase of 5.26% in body drag. At a high angle of attack, while body elongation causes a 4.34% drag increase, body expansion causes a 10.80% drag increase. Therefore, in the subsonic regime, while body expansion and elongation at a low angle of attack cause an equal drag increase, elongation at a high angle of attack provides a significant advantage over widening. In the supersonic regime, while a 270-mm (15%) elongation in the fuselage at low angles of attack causes a 2.43% increase in body drag, the 6.51-mm widening of the radius of the center body cross-section causes a 14.60% increase in body drag. At a high angle of attack, while body elongation causes a 6.39% drag increase, center body widening causes a 9.88% body drag increase. As seen from Fig. 9, body elongation is more advantageous than body enlargement at both low and high angles of attack in both flight regimes. This advantage becomes dominant at high angles of attack, especially in the subsonic regime, and at low angles of attack in the supersonic regime. To increase the volume of the aircraft center body by 11451 cm<sup>3</sup>, an extension of the center body length by 450 mm or an increase in its radius by 10.62 mm is required. The effect of these geometry changes, which will provide the same volume increase, on body drag is calculated separately and shown in Fig. 10.

To increase the volume of the aircraft center body by 16032 cm<sup>3</sup>, an extension of the center body length by 630 mm or an increase in its radius by 14.57 mm is required. The effect of these geometry changes, which will provide the same volume increase, on body drag is calculated separately and shown in Fig. 11.

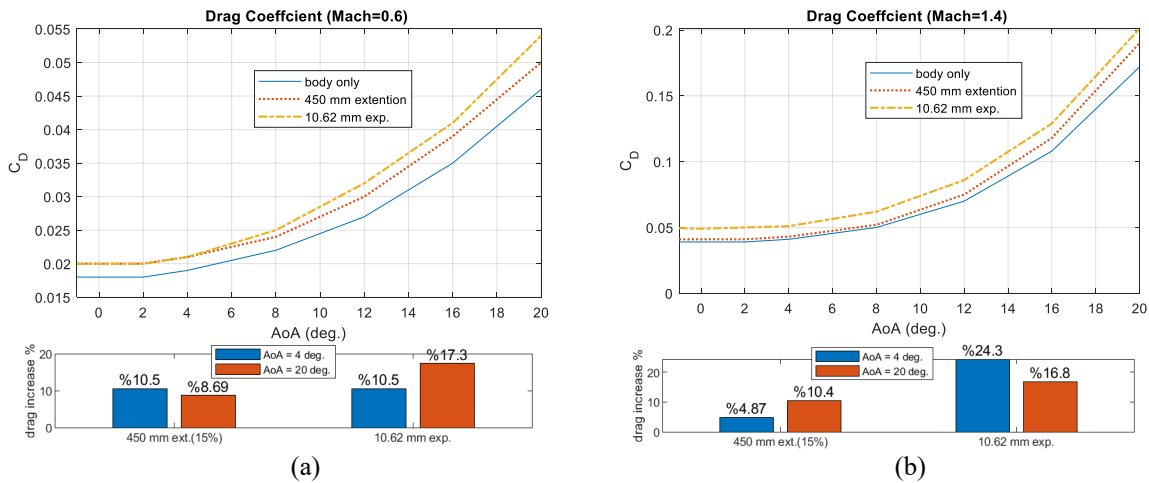


**Figure 10.** The influence of the 450-mm extension of the body length or the 10.62-mm expansion of the cross-section radius on the body-only drag coefficient in: (a) Subsonic regime (Mach=0.6), (b) Supersonic regime (Mach=1.4)

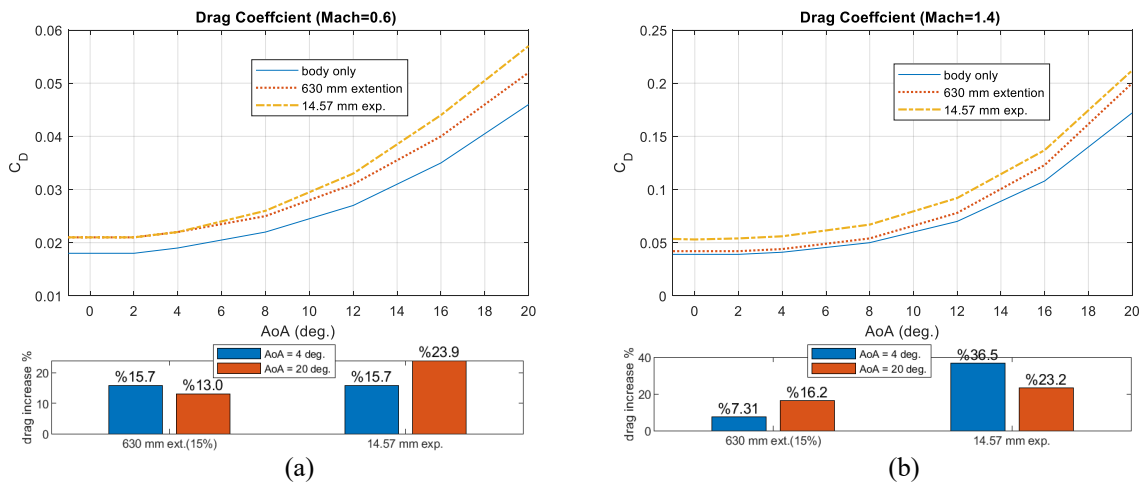


**Figure 11.** The influence of the 630-mm extension of the body length or the 14.57-mm expansion of the cross-section radius on the body-only drag coefficient in: (a) Subsonic regime (Mach=0.6), (b) Supersonic regime (Mach=1.4)

The results in Figs. 10 and 11 are in parallel with Fig. 9. In both flight regimes, center body elongation at low and high angles of attack outperforms its widening. This advantage becomes dominant at high angles of attack, especially in the subsonic regime, and at low angles of attack in the supersonic regime.

#### 4. Conclusions

In this study, a practical and low-cost approach is developed to predict the drag cost of volume increase in various ways during the aircraft design process using MATLAB and DATCOM software. The lengthening of the center body and the increase in its radius are considered the same volume increases. Owing to this approach, body drag coefficient values are calculated and plotted in seconds for both subsonic and supersonic regimes for 3 different volume increases with 6 different geometry changes. According to the results, the effect of the center body percent elongation and the percentage increase of its cross-section radius on the body drag coefficient is expressed as second-order equations for both low and high angles of attack. These equations can be used to give

quick ideas for aircraft with similar geometries and missions, especially at the early design stages. The 35% elongation of the center body results in a 16.2% increase in the maximum drag coefficient, while the 16.16 % increase in the center body section radius results in a 36.5% increase in the maximum drag coefficient. This would roughly mean the need for an engine producing 16.2% and 36.5% more thrust, respectively, than intended to be used in the design. It can be inferred from the results that when an increase in the volume is required, increasing the center body length causes less body drag increase according to increasing its section radius. While it is already expected that elongation causes more drag than expansion, the magnitude of the drag difference is also important. If the drag disadvantage caused by widening will not cause a change in engine selection in the aircraft design, body widening may also be preferred due to the advantage it provides in terms of placement in the body. Therefore, it requires such a comparative analysis approach. The systematic approach made on the aircraft fuselage in this study can also be used to analyze the effects of changes on the aircraft's surfaces such as wings and tail. Especially the performance effects of aircraft in the morphing aircraft category, which can change their geometry during flight, can be analyzed using the same approach.

### Code Availability

The MATLAB code used in this study is available at:  
<https://drive.google.com/drive/folders/1TxFMq3h2x67A3-FDsiyNfVv6s06zx-3b?usp=sharing>

### References

- [1] Wu H, Gao M, Song X, Xu J, Wang Y, Zhao J. Accuracy Analysis of Aerodynamic Calculation of 2-Dimensional Trajectory Correction Projectile Based on DATCOM. *Curr Eng Lett Rev* 2019; 27 (4).
- [2] Sun D, Wu H, Zhu R, Hung LC. Development of Micro Air Vehicle Based on Aerodynamic Modeling Analysis in Tunnel Tests. In: *Proceedings of the 2005 IEEE International Conference on Robotics and Automation*; Barcelona, Spain, 2005, pp. 2235-2240.
- [3] Haque AU, Asrar W, Omar AA, Sulaiman E, Ali MJS. Preliminary Aerodynamic and Static Stability Analysis for Hybrid Buoyant Aerial Vehicles at Low Speeds Using Digital DATCOM. *Can Aeronaut Space J* 2015; 61 (3).
- [4] Sahu J. Time-Accurate Aerodynamic Modeling of Synthetic Jets for Projectile Control. In: *2004 Users Group Conference (DOD UGC'04)*, Williamsburg, VA, USA, 2004. pp. 144–150.
- [5] Ahmad M, Hussain ZL, Shah SIA, Shams TA. Estimation of Stability Parameters for Wide Body Aircraft Using Computational Techniques. *Appl Sci-Basel* 2021; 11 (5), 2087.
- [6] Anderson, J. D. *Computational Fluid Dynamics*. McGraw-Hill Professional: New York, NY, 1995.
- [7] Melin T. *User's Guide and Reference Manual for Tornado*. Royal Inst of Technology KTH: Stockholm, Sweden, 2000.
- [8] Sooy TJ, Schmidt RZ. Aerodynamic Predictions, Comparisons, and Validations Using Missile DATCOM (97) and Aeroprediction 98 (AP98). *J Spacecr Rockets* 2005; 42 (2), 257–265.
- [9] Zhang W, Wang Y, Liu Y. Aerodynamic Study of Theater Ballistic Missile Target, *Aerosp Sci Technol* 2013; 24 (1), 221–225.
- [10] Grasmeyer J. *Stability and Control Derivative Estimation and Engine-Out Analysis*, Virginia Polytechnic Institute and State University, Blacksburg, VA, USA, 1998.
- [11] Anton N, Botez R, Popescu D. New Methodologies for Aircraft Stability Derivatives Determination from its Geometrical Data. In: *AIAA Atmospheric Flight Mechanics Conference*; American Institute of Aeronautics and Astronautics: Reston, Virginia, 2009.
- [12] Maurice AF. *Aerodynamic Performance Predictions of a SA-2 Missile Using Missile DATCOM*. M.Sc. Thesis, University of Florida, 2009.
- [13] Blake WB. *Missile DATCOM: 1997 Status and Fluent Plans*. American Institute of Aeronautics and Astronautics 1997, AIAA-97-2280, 538–548.
- [14] Nguyen NV, Kim WS, Lee JW, Byun YH. Validations, Prediction, and Aerodynamic Optimization of Short and Medium Range Missile Configurations. In: *KSAS-JSASS Joint International Symposium 2008*, 146–152.
- [15] Shistik E, Sigal A. The Interaction between Canards and Thick Bodies: Implementation in the Missile Datcom Code. In *20th AIAA Applied Aerodynamics Conference*; American Institute of Aeronautics and Astronautics: Reston, Virginia, 2012.
- [16] Nicolosi F, Vecchia PD, Ciliberti D. An Investigation on Vertical Tailplane Contribution to Aircraft Sideforce. *Aerosp Sci Technol* 2013; 28 (1), 401–416.
- [17] Bakar MRA, Basuno B, Hasan S. Aerodynamics Analysis on Unsymmetrical Fuselage Models. *Applied Mechanics and Materials* 2013; 315, 273–277.
- [18] Li T, Yan P, Jiang RM, Zhou J. Calculation and Analysis of High-Speed Missile's Aerodynamic Characteristic with Asymmetric Morphing Wings. *Journal of Ordnance Equipment Engineering* 2017; 2017, 51–56.

- [19] Zhang GP, Duan ZY, Liao ZZ, Zhang Y. Multi-Body Dynamics of Tactical Missile with Morphing Wing. *Journal of Projectile, Rockets, Missile and Guidance* 2011; 31, 149–151, 158.
- [20] Wei DH, Chen WC, Li NY, Xu P. Morphing Theory and Control Approaches of a Morphing Missile. *Tactical Missile Technology* 2016; 2, 10–15.
- [21] Zheng MM. Modeling and Flight Control of the Variable-Sweep Aircraft in the Whole Morphing. Nanjing University of Aeronautics and Astronautics the Graduate School, 2015.
- [22] Guo SJ. Research on Cooperative Control of the Morphing Aircraft. Nanjing University of Aeronautics and Astronautics the Graduate School College of Automation Engineering, 2012.
- [23] Yan X, Zhu J, Kuang M, Wang X. Aerodynamic Shape Optimization Using a Novel Optimizer Based on Machine Learning Techniques. *Aerosp Sci Technol* 2019; 86, 826–835.
- [24] Nahon M. Determination of Undersea Vehicle Hydrodynamic Derivatives Using the USAF Datcom. In: *Proceedings of OCEANS '93*, Victoria, BC, Canada, 1993.
- [25] Rauf A, Zafar MA, Ashraf Z, Akhtar H. Aerodynamic Modeling and State-Space Model Extraction of a UAV Using DATCOM and Simulink. In: *2011 3rd International Conference on Computer Research and Development*, Shanghai, China, 2011.
- [26] Triputra FR, Trilaksono BR, Sasongko RA, Dahsyat M. Longitudinal Dynamic System Modeling of a Fixed-Wing UAV towards Autonomous Flight Control System Development: A Case Study of BPPT Wulung UAV Platform. In *2012 International Conference on System Engineering and Technology (ICSET)*, Bandung, Indonesia, 2012, pp. 1-6.
- [27] Jamil MA, Ahsan M, Ahsan MJ, Choudhry MA. Time Domain System Identification of Longitudinal Dynamics of a UAV: A Grey Box Approach. In: *2015 International Conference on Emerging Technologies (ICET)*, Peshawar, Pakistan, 2015, pp. 1-6.
- [28] Bashir M, Khan SA, Udayagiri L, Noor A. Dynamic Stability of Unguided Projectile with 6-DOF Trajectory Modeling. In: *2017 2nd International Conference for Convergence in Technology (I2CT)*, Mumbai, India, 2017, pp. 1002-1009.
- [29] Jeevan HL, Narahari HK, Sriram AT. Development of Pitch Control Subsystem of Autopilot for a Fixed Wing Unmanned Aerial Vehicle. In: *2018 2nd International Conference on Inventive Systems and Control (ICISC)*, Coimbatore, India, 2018, pp. 1233-1238.
- [30] Yang J, Wen L, Jiang B, Wang Z. Dynamic Modeling and Flight Simulation of a Folding Wing-Tip UAV. In: *2020 Chinese Control And Decision Conference (CCDC)*, Hefei, China, 2020, pp. 1814-1819.
- [31] Turevskiy A, Gage S, Buhr C. Model-Based Design of a New Light-Weight Aircraft. In: *AIAA Modeling and Simulation Technologies Conference and Exhibit*; American Institute of Aeronautics and Astronautics: Reston, Virginia, 2007.
- [32] Anton N, Popescu D, Botez RM. Estimation of Stability Derivatives from Aircraft Geometrical Data for Use in Simulator Applications, Conference: American Romanian Academy ARAAt: Boston, MI, USA, 2007.
- [33] Raymer DP. *Aircraft Design: A Conceptual Approach*; American Institute of Aeronautics & Astronautics: Reston, VA, 2012.